Analysis of Rocker Mechanism for Automobile Windscreen Wiper Applications *(pp. 13-54)*

Christopher Okechukwu Izelu,
Department of Mechanical Engineering, Faculty of Engineering, Nigerian Defence Academy,
Kaduna, Nigeria

Abstract: This paper presents the use of a computer oriented numerical approach in the characterization of the crank-double rocker mechanism of automobile windscreen wipers. The vector loop-closure technique, Newton-Raphson method for solution of nonlinear systems, and the concepts of velocity coefficients and velocity coefficient derivatives are used to formulate angular position, velocity and acceleration models for the kinematic analysis. The generalized energy-based equation of motion for single degree of freedom planar systems, the principles of virtual work, and those of force and moment equilibrium are used to formulate output torque, pin-joint or internal and reactive force models for the kinetostatic analysis. The effects of input speed, input torque and wiper contact friction on power transmission capability of the mechanism are studied in numerical experiments with the derived models, using ANOVA with repeated measures to establish these effects. It is found that the numerical models described, to acceptable levels, the kinematic and kinetostatic characteristics of the mechanism. The oscillatory or rocking motion is characteristic of the rockers, while the combined oscillatory and reciprocating motion is characteristic of the connecting links. Also, the input speed, input torque and friction factor have significant influence on the power transmission capability of first loop of the mechanism, whereas, only the friction factor has significant influence on the power transmission capability of second loop of the mechanism. The results showed that the derived models are quite suitable for the purpose of design and analysis of the mechanism and its extensions.

Key words: kinematic analysis, kinetostatic analysis, mechanism, linkages, function generation, motion transformation and   power transmission

NOTATION: The following notations are used.

q	Input crank angular position (rad)
$\dot{q}$	Input crank angular speed (rad/s)
$\ddot{q}$	Input crank angular acceleration (rad/s^2)
$\alpha,\ \beta$	Fixed angles (rad)
A	Angular position for the other links (rad)
$\dot{A}$	Angular velocity for the other links (rad/s)
$\ddot{A}$	Angular acceleration for the other links (rad/s^2)

K	Velocity coefficient for the other links (---)
L	Velocity coefficient derivative for the other links (---)
x, y	Cartesian coordinate directions
X, Y	Components of the mass center position (m) in the coordinate directions
$\dot{X}, \dot{Y}$	Components of the mass center velocity (m/s) in the coordinate directions
$\ddot{X}, \ddot{Y}$	Components of the mass center velocity (m/s^2) in the coordinate directions
V	Linear velocity of connecting links (m/s)
C	Linkage dimension (m)
M	Linkage Mass (kg)
I	Linkage moment of Inertia about axes of rotation or mass centre ($kg\ m^2$)
T	Input, output and contact friction torque (Nm)
TR	Transmission ratio (---)

m	Contact friction factor between the windscreen and wiper blade (---)
η	Power loss factor or transmission efficiency (---)

1   INTRODUCTION

The use of mechanisms and linkages for function, motion and path generation in any dynamical mechanical systems requires that the designer understand their kinematic and kinetostatic characteristics and function to be able to determine how the various components are stressed, the magnitude of these stresses, and the optimum size and shape of the components that would withstand the operating loads. The kinematic characteristics refer to such variables as position, velocity and acceleration, which describe the motion of the system without consideration of the forces and moments responsible for the motion. The kinetostatic characteristics, on the other hand, refer to such variables as output torque, pin-joint or internal and reactive forces, which may operate under static or dynamic conditions, and are responsible for the motion of the system. The knowledge of these properties of mechanisms and linkages is vital to mechanical systems designers, who may need such scarce technical information to be able to determine the operating stresses and suitable component sizes, and then, come up with rational and satisfactory designs that would effectively and economically deliver desired services, and yet, stand the test of time.

Previous works on the design and analysis of mechanisms and linkages of dynamical mechanical systems have proposed a number of concepts and approaches, including graphical, analytical and numerical methods, for describing the kinematic and kinetostatic properties of these systems. For instance, some of these concepts and approaches and their uses have been directly or indirectly discussed in the books of Paul (1975); Erdman et al (1984a, 1984b); and in the works of Berkof et al (1971); Lowen et al (1971); Erdman et al (1972); Berkof (1979); Bahgat (1976); Wehage et al, (1982); Sohoni et al (1982); Singhal et

al1(983); Doughty (1988); Nelson et al (1999); Zoskowicz et al (1999); Cheng et al (2006); Wang (2008), and Nagchaudhuri (2008).

The attractiveness of these concepts and methods of analysis has been reckoned with in design and analysis of mechanisms and linkages and in the development of the most related offline and online analysis software packages with regards to their excellent analytical capabilities. However, their application with regards to the description of kinematic and kinetostatic characteristics of some very important mechanisms and linkages deserves further attention in order to enhance understanding of these mechanisms and ability of designers to use the developed software packages in obtaining applicable design data and interpreting the behaviour of these mechanisms. In view of the observed deficiency in application of the developed analytical tools and of computational reasons, the numerical approach of Doughty, 1988 has successfully been used in the works of Izelu, (2000, 2002) to characterize the external rotary Geneva mechanism (Izelu, 2000), and also evaluate its power transmission capabilities with regards to the effect of its size, input torque and input speed (Izelu, 2002). An extension of these efforts, therefore, is given in this work with interest in the kinematic and kinetostatic characterization and in evaluation of the power transmission capability of the crank-double rocker mechanism for automobile windscreen wiper applications, a case of Honda Accord, 92-model salon car and for many other similar mechanical system applications that might be of interest to the designers and fabricators at local and global levels. The fact that no documented evidence of previous and similar study of the mechanism is found has also motivated this study. However, crank-rocker four-bar linkages have been studied due to their wide application in mechanical systems, but with different approaches and for different applications not as cascaded in the case studied.

The undertaken numerical analysis of the crank-double rocker mechanism for wind-screen wiper applications involves the use of vector loop-closure technique, Newton-Raphson method for solution of nonlinear systems, and the concepts of velocity coefficients and velocity coefficient derivatives to formulate models for the kinematic analysis (Doughty, 1988). The generalized energy-based equation of motion, known as the Eksergians equation of motion, the principles of virtual work, and those of the force and moment equilibrium, on the other hand, were used to formulate models for the kinetostatic analysis. One advantage of the method is that velocity and acceleration are expressed as velocity coefficients and velocity coefficient derivatives, respectively. These coefficients are the ratio of linkage motion to that of the crank, and consequently, have values that are uninfluenced by the crank motion except by its position as it rotates about its axis. The numerical data, required to test the accuracy, efficacy and utility of the models, to characterize the mechanism and to evaluate the capacity of the mechanism for effective motion transformation and power transmission are obtained through numerical experiments with the models conducted in MS Excel environment.

2   METHODOLOGY

2.1   Geometry of the Mechanism

The crank-double rocker mechanism is a two loop, single degree of freedom, four-bar linkages, whose output motions at the rockers are oscillatory or simply a rocking type of motion under single rotational input motion. It is a function generator having linkages in which the relative motions, forces or moments in links connected to the ground or the fixed frame are of interest (Erdman et al, 1984a, 1984b). In other words, it is designed to convert or transform the rotational input motion to oscillatory or rocking output motions, and to transmit desired output torque from given input torque. As used in wind-screen wiper of Honda Accord 92 model salon car (see appendix), the space or kinematics diagram showing the various components of the mechanism is given in Figure 1.

As shown in Figure 1, the mechanism consists of two four-bar linkages, which in principle, are coupled together by a triangular link denoted as rocker 1 (bo_2c). The first loop of the mechanism, or the first four-bar linkage consists of the fixed link 1 (o_1o_2), crank (o_1a), connecting link 1 (ab) and part of the rocker 1 (bo_2). The crank receives input rotational motion from the shaft of a worm geared electric motor, and transfers this motion through translating and oscillating connecting link 1 to oscillating or rocking rocker 1 while they are supported on the fixed link 1. The second loop of the mechanism, or the second four-bar linkage consists of the fixed link 2 (o_2o_3), part of the rocker 1 (o_2c), connecting link 2 (cd) and rocker 2 (o_3a). The oscillating rocker 1 transfers its motion to oscillating rocker 2 through oscillating and reciprocating connecting link 2, while they are supported on the fixed link 1.   The fixed link 1 and 2 are integral part of the fixed frame which provides overall support for the mechanism.
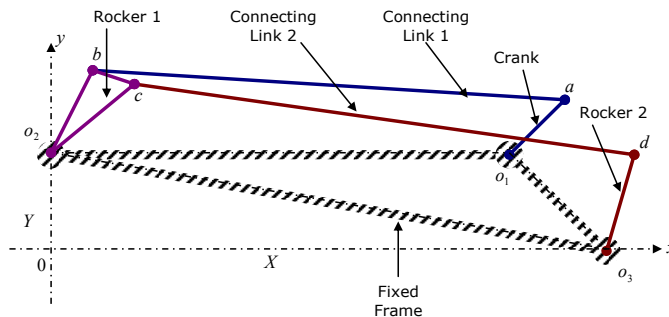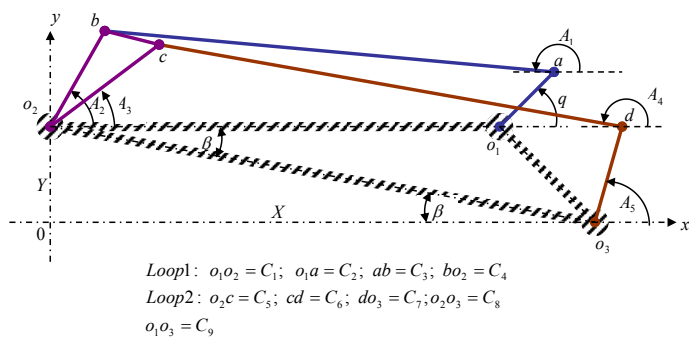

Figure 1: Components of the dual crank-rocker mechanism

The analysis assumes that the linkages of the mechanism are rigid and perfectly elastic and that they perform their respective function of motion transformation and power transmission without losses of power due elastic deflection of the linkages, except by friction at pin-joints and at the contact between the wiper and the windscreen. It also assumed that the joints are perfect and revolute, and that the resisting torque due to pin-joint and wiper-windscreen contact friction is directly proportional to the applied torque, and that the input torque and speed are continuous and constant. Note that the variety in its function (i.e. intermittent, slow and fast sweep of wiper blades) to suit different conditions of rainfall is not mechanically activated, but through electronics control of electric motor operation. Consideration of the electronic control mechanism is outside the scope of this work.

2.2   Kinematic Models

The linear kinematic models include the position, velocity and acceleration models. These are mathematical expressions derived as functions of crank rotation or angular position based on the system geometry (Figure 2), such that, when evaluated at different angular positions of the crank would yield, the angular positions, angular velocities and angular accelerations that determine the kinematic characteristics of other links of the mechanism. These models are derived using Doughty's numerical approach (Doughty, 1988) as follows:

$Loop1:\ o_1o_2 = C_1;\ o_1a = C_2;\ ab = C_3;\ bo_2 = C_4$
$Loop2:\ o_2c = C_5;\ cd = C_6;\ do_3 = C_7; o_2o_3 = C_8$
$o_1o_3 = C_9$

Figure 2: Kinematic diagram for the dual crank-rocker mechanism

(a) **Position Model**: The position model for kinematics of the mechanism is derived using the vector loop closure technique (Doughty, 1988). From the kinematic diagram given in Figure 2, the vector loop equations for the two loops of the mechanism are given as,

$$\vec{C}_1 + \vec{C}_2 + \vec{C}_3 + \vec{C}_4 = 0 \tag{1}$$

$$\vec{C}_5 + \vec{C}_6 + \vec{C}_7 + \vec{C}_8 = 0 \tag{2}$$

Equations (1) and (2) govern the kinematics of the mechanism. The scalar forms of these equations may be writing direct from Fig. 3 as,

$$C_1 + C_2 \cos q - C_3 \cos A_1 + C_4 \cos A_2 = 0 \tag{3}$$

$$C_2 \sin q + C_3 \sin A_1 + C_4 \sin A_2 = 0 \tag{4}$$

$$C_5 \cos A_3 + C_6 \cos A_4 + C_7 \cos A_5 - C_8 \cos \beta = 0 \tag{5}$$

$$C_5 \sin A_3 - C_6 \sin A_4 + C_7 \sin A_5 + C_8 \sin \beta = 0 \tag{6}$$

The constraint scalar equation couples the vector loop equations and it is given as,

$$\alpha - A_2 + A_3 = 0 \tag{6}$$

The scalar loop equations together with the constraint equation are non-linear systems, whose solutions constitute the position model. The solutions may be obtained using Newton-Raphsons method (Doughty, 1988; Chapra et al, 1998; Cheney et al, 1990; Rajasekaran, 2003) for non linear systems as follows:

The scalar loop and constraint equations are first rewritten as,

$$f_1 = f(q, A_1, A_2, A_3, A_4, A_5) = C_1 + C_2 \cos q - C_3 \cos A_1 + C_4 \cos A_2 \tag{7}$$

$$f_2 = f(q, A_1, A_2, A_3, A_4, A_5) = C_2 \sin q + C_3 \sin A_1 + C_4 \sin A_2 \tag{8}$$

$$f_3 = f(q, A_1, A_2, A_3, A_4, A_5) = C_5 \cos A_3 + C_6 \cos A_4 + C_7 \cos A_5 - C_8 \cos \beta \tag{9}$$

$$f_4 = f(q, A_1, A_2, A_3, A_4, A_5) = C_5 \sin A_3 - C_6 \sin A_4 + C_7 \sin A_5 + C_8 \sin \beta \tag{10}$$

$$f_5 = f(q, A_1, A_2, A_3, A_4, A_5) = \alpha - A_2 + A_3 \tag{11}$$

The $5x1$ solution vector of unknown position variables and the $5x1$ residual vector of scalar functions may, respectively, be defined as,

$$\{S_k\} = \{A_1 \quad A_2 \quad A_3 \quad A_4 \quad A_5\}^T \text{ and } \{F(S_k)\} = \{f_1 \quad f_2 \quad f_3 \quad f_4 \quad f_5\}^T \tag{12}$$

Therefore, using these definitions and the concept of Jacobian matrix, $[J(S_k)]$, the non-linear system may be linearized and the resulting linear system written for the position variables as,

$$[J(S_k)]\{\Delta S\} = -\{F(S_k)\} \tag{13}$$

Solving the linear system iteratively for $\{\Delta S\}$, therefore yields,

$$\{\Delta S\} = -[J(S_k)]^{-1}\{F(S_k)\} \tag{14}$$

For the next iteration, the following is used,

$$\{S_{k+1}\} = \{S_k\} + \{\Delta S\} \tag{15}$$

Note that, for the system studied, the obtained Jacobian matrix is given as,

$$[J(S_k)] = \left[\frac{\partial f}{\partial S_k}\right] = \begin{bmatrix} C_3 \sin A_1 & -C_4 \sin A_2 & 0 & 0 & 0 \\ C_3 \cos A_1 & C_4 \cos A_2 & 0 & 0 & 0 \\ 0 & 0 & -C_5 \sin A_3 & -C_6 \sin A_4 & -C_7 \sin A_5 \\ 0 & 0 & C_5 \cos A_3 & -C_6 \cos A_4 & C_7 \cos A_5 \\ 0 & -1 & 1 & 0 & 0 \end{bmatrix} \tag{16}$$

The obtained residual vector is given as,

$$\{F(S_k)\} = \begin{Bmatrix} C_1 + C_2 \cos q - C_3 \cos A_1 + C_4 \cos A_2 \\ C_2 \sin q + C_3 \sin A_1 + C_4 \sin A_2 \\ C_5 \cos A_3 + C_6 \cos A_4 + C_7 \cos A_5 - C_8 \cos \beta \\ C_5 \sin A_3 - C_6 \sin A_4 + C_7 \sin A_5 + C_8 \sin \beta \\ \alpha - A_2 + A_3 \end{Bmatrix} \tag{17}$$

For kinematics of linkage mass centers [Doughty, 1988], expressions for the scalar position equations are given as follows:

For the **crank**,

$$X_2 = U_2 \cos q \quad \text{and} \quad Y_2 = U_2 \sin q \tag{18}$$

For the **connecting link 1**,

$$X_3 = C_2 \cos q - U_3 \cos A_1 \text{ and } Y_3 = C_2 \sin q + U_3 \sin A_1 \tag{19}$$

For the **rocker 1a**,

$$X_4 = U_4 \cos A_2 \text{ and } Y_4 = U \sin A_2 \tag{20}$$

For the **rocker 1b**,

$$X_5 = U_5 \cos A_3 \text{ and } Y_5 = Y + U_5 \sin A_3 \tag{21}$$

For the **connecting link 2**,

$$X_6 = C_5 \cos A_3 + U_6 \cos A_4 \text{ and } Y_6 = Y + C_5 \sin A_3 - U_6 \sin A_4 \tag{22}$$

For the **rocker 2**,

$$X_7 = U_7 \cos A_5 \text{ and } Y_7 = U_7 \sin A_5 \tag{23}$$

(b) **Velocity Model**: The velocity model for kinematics of the mechanism is obtained from the scalar velocity loop equations, through the derivatives of the scalar position loop and constraint equations with respect to time (Doughty, 1988). Expressed in matrix form, the derivatives of the scalar position loop and constraint equations give a linear system of the form,

$$\left[\frac{\partial f}{\partial S}\right]\{\dot{S}\} = -\dot{q}\left\{\frac{\partial f}{\partial q}\right\} \text{ or } [J(S)]\{\dot{S}\} = -\dot{q}\{F(q)\} \tag{24}$$

Alternatively, rearranging the system, in terms of the velocity coefficients vector, gives,

$$[J(S)]\frac{\dot{S}}{\dot{q}} = -\{F(q)\} ; \quad [J(S)]\{K_s\} = -\{F(q)\} \text{ or } \{K_s\} = -[J(S)]^{-1}\{F(q)\} \tag{25}$$

Note that, the velocity vector, velocity coefficient vector, and the residual function of crank position are respectively defined as,

$$\{\dot{S}\}=\frac{\partial S}{\partial t}=\{\dot{A}_1 \quad \dot{A}_2 \quad \dot{A}_3 \quad \dot{A}_4 \quad \dot{A}_5\}^T \quad \{K\}=\frac{\dot{S}}{\dot{q}}=\{K_1 \quad K_2 \quad K_3 \quad K_4 \quad K_5\}^T$$
, and

$$\{F(q)\}=\left\{\frac{\partial f}{\partial q}\right\}=\{-C_2 \sin q \quad C_2 \cos q \quad 0 \quad 0 \quad 0\}^T$$

(26)

The solution of (25) by any known matrix method (Chapra et al, 1998; Cheney et al, 1990; Rajasekaran, 2003) yields the velocity coefficients for the various links of the mechanism.

For kinematics of the linkage mass centers (Doughty, 1988), expressions for the velocity coefficients, obtained from the derivatives of the scalar position equations with respect to time, are given as follows:

For the **crank,**

$$\dot{X}_2 =-\dot{q}U_2 \sin q = \dot{q}K_{x2}, \text{ or } K_{x2}=\dot{X}_2/\dot{q}=-U_2 \sin q$$

(27)

$$\dot{Y}_2 = \dot{q}U_2 \sin q = \dot{q}K_{y2}, \text{ or } K_{y2}=\dot{Y}_2/\dot{q}=U_2 \cos q$$

(28)

For the **connecting link** 1:

$$\dot{X}_3 =-\dot{q}C_2 \sin q + \dot{A}_1 U_3 \sin A_1 = -\dot{q}C_2 \sin q + \dot{q}K_1 U_3 \sin A_1$$
$$=\dot{q}(-C_2 \sin q + K_1 U_3 \sin A_1)=\dot{q}K_{x3} \ or$$
$$K_{x3} = \dot{X}_3/\dot{q} = -C_2 \sin q + K_1 U_3 \sin A_1$$

(29)

$$\dot{Y}_3 =\dot{q}C_2 \cos q + \dot{A}_1 U_3 \cos A_1 = \dot{q}C_2 \cos q + \dot{q}K_1 U_3 \cos A_1$$
$$=\dot{q}(C_2 \cos q + K_1 U_3 \cos A_1)=\dot{q}K_{y3}; \ or$$
$$K_{y3} = \dot{Y}_3/\dot{q} = C_2 \cos q + K_1 U_3 \cos A_1$$

(30)

For the **rocker 1a**:

$$\dot{X}_4 =-\dot{A}_2 U_4 \sin A_2 = -\dot{q}K_2 U_4 \sin A_2 = \dot{q}K_{x4} \text{ or } K_{x4}=\dot{X}_4/\dot{q}=-K_2 U_4 \sin A_2$$

(31)

$$\dot{Y}_4 =\dot{A}_2 U_4 \cos A_2 = \dot{q}K_2 U_4 \cos A_2 = \dot{q}K_{y4} \text{ or } K_{y4}=\dot{Y}_4/\dot{q}=K_2 U_4 \cos A_2$$

(32)

For the **rocker 1b**:

$$\dot{X}_5 = -\dot{A}_3 U_5 \sin A_3 = -\dot{q} K_3 U_5 \sin A_3 = \dot{q} K_{x5} \text{ or } K_{x5} = \dot{X}_5/\dot{q} = -K_3 U_5 \sin A_3 \tag{33}$$

$$\dot{Y}_5 = \dot{A}_3 U_2 \cos A_3 = \dot{q} K_3 U_5 \cos A_3 = \dot{q} K_{y5} \text{ or } K_{y5} = \dot{Y}_5/\dot{q} = K_3 U_5 \cos A_3 \tag{34}$$

For the **connecting link 2**:

$$\begin{aligned}
\dot{X}_6 &= -\dot{A}_3 C_5 \sin A_3 - \dot{A}_4 U_6 \sin A_4 = -\dot{q} K_3 C_5 \sin A_3 - \dot{q} K_4 U_6 \sin A_4 \\
&= \dot{q}\left(-K_3 C_5 \sin A_3 - K_4 U_6 \sin A_4\right) = \dot{q} K_{x6}; \; or \\
K_{x6} &= \dot{X}_6/\dot{q} = -K_3 C_5 \sin A_3 - K_4 U_4 \sin A_4
\end{aligned} \tag{35}$$

$$\begin{aligned}
\dot{Y}_6 &= \dot{A}_3 C_5 \cos A_3 - \dot{A}_4 U_6 \cos A_4 = \dot{q} K_3 C_5 \cos A_3 - \dot{q} K_4 U_6 \cos A_4 \\
&= \dot{q}\left(K_3 C_5 \cos A_3 - K_4 U_6 \cos A_4\right) = \dot{q} K_{y6}; \; or \\
K_{y6} &= \dot{Y}_6/\dot{q} = K_3 C_5 \cos A_3 - K_4 U_4 \cos A_4
\end{aligned} \tag{36}$$

For the **rocker 2**:

$$\dot{X}_7 = -\dot{A}_5 U_7 \sin A_5 = -\dot{q} K_5 U_7 \sin A_5 = \dot{q} K_{x7}; \text{ or } K_{x7} = \dot{X}_7/\dot{q} = -K_5 U_7 \sin A_5 \tag{37}$$

$$\dot{Y}_7 = \dot{A}_5 U_7 \cos A_5 = \dot{q} K_5 U_7 \cos A_5 = \dot{q} K_{y7}; \text{ or } K_{y7} = \dot{Y}_7/\dot{q} = K_5 U_7 \cos A_5 \tag{38}$$

(c) **Acceleration Model**: The acceleration model for kinematics of the mechanism is obtained from the scalar acceleration loop equations, through second derivatives of the scalar position loop and constraint equations with respect to time (Doughty, 1988). That is, in terms of the velocity coefficients, the velocity relation and its derivative with respect to time are respectively, given as,

$$\{\dot{S}\} = \dot{q}\{K_s\} \text{ and } \{\ddot{S}\} = \ddot{q}\{K_s\} + \dot{q}^2 \frac{d(\{K_s\})}{dq} = \ddot{q}\{K_s\} + \dot{q}^2\{L_s\} \tag{39}$$

Note that, the acceleration, velocity coefficients and velocity coefficient derivative vectors are, respectively, defined as,

$$\{\ddot{S}\} = \left\{\ddot{A}_1 \quad \ddot{A}_2 \quad \ddot{A}_3 \quad \ddot{A}_4 \quad \ddot{A}_5\right\}^T; \quad \{K_s\} = \left\{\frac{\dot{S}}{\dot{q}}\right\} = \left\{K_1 \quad K_2 \quad K_3 \quad K_4 \quad K_5\right\}^T; \text{ and}$$

$$\{L_s\} = \{L_1 \quad L_2 \quad L_3 \quad L_4 \quad L_5\}^T \tag{40}$$

The velocity coefficient derivatives vector, $\{L_s\}$, is obtained by solving the linear system, given as,

$$[J(S)]\{L\} = -\{\xi\} \quad \text{or} \quad \{L\} = [J(S)]^{-1}\{\xi\} \tag{41}$$

Note that,

$$\{\xi\} = \frac{d\{\partial f/\partial q\}}{dq} + \{K\}^2 \frac{d[\partial f/\partial S]}{dS} = \{\varsigma\} + [\zeta]\{K\}^2 \tag{42}$$

But,

$$\{\varsigma\} = \frac{d\{\partial f/\partial q\}}{dq} = \{-C_2 \cos q \quad -C_2 \sin q \quad 0 \quad 0 \quad 0\}^T \tag{43}$$

and

$$[\zeta] = \frac{d[\partial f/\partial S]}{dS} = \begin{bmatrix} C_3 \cos A_1 & -C_4 \cos A_2 & 0 & 0 & 0 \\ -C_3 \sin A_1 & -C_4 \sin A_2 & 0 & 0 & 0 \\ 0 & 0 & -C_5 \cos A_3 & -C_6 \cos A_4 & -C_7 \cos A_5 \\ 0 & 0 & -C_5 \sin A_3 & C_6 \sin A_4 & -C_7 \sin A_5 \\ 0 & 0 & 0 & 0 & 0 \end{bmatrix} \tag{44}$$

Therefore, using (43) and (44) in (42), and simplifying, yields,

$$\{\xi\} = \begin{Bmatrix} -C_2 \cos q + C_3 K_1^2 \cos A_1 - C_4 K_2^2 \cos A_2 \\ -C_2 \sin q - C_3 K_1^2 \sin A_1 - C_4 K_2^2 \sin A_2 \\ -C_5 K_3^2 \cos A_2 - C_6 K_4^2 \cos A_4 - C_7 K_5^2 \cos A_5 \\ -C_5 K_3^2 \sin A_2 + C_6 K_4^2 \sin A_4 - C_7 K_5^2 \sin A_5 \\ 0 \end{Bmatrix} \tag{45}$$

The solution of (41) by any known matrix method (Chapra et al, 1998; Cheney et al, 1990; Rajasekaran, 2003) yields the velocity coefficient derivatives for the various links of the mechanism.

For kinematics of the linkage mass centers (Doughty, 1988), expressions for the velocity coefficient derivatives, obtained from the second derivates of the scalar position equations with respect to time, are given as follows:

For the **crank**,

$$\ddot{X}_2 = -\ddot{q}U_2 \sin q - \dot{q}^2 U_2 \cos q = \ddot{q}K_{x2} + \dot{q}^2 L_{x2}$$

where, $K_{x2} = -U_2 \sin q$ and $L_{x2} = -U_2 \cos q$ $\hspace{2cm}$ (46)

$$\ddot{Y}_2 = \ddot{q}U_2 \cos q - \dot{q}^2 U_2 \sin q = \ddot{q}K_{y2} + \dot{q}^2 L_{y2}$$

where, $K_{y2} = U_2 \cos q$ and $L_{y2} = -U_2 \sin q$ $\hspace{2cm}$ (47)

For the **connecting link 1**,

$$\ddot{X}_3 = \ddot{q}K_{x3} + \dot{q}L_{x3}$$

where, $K_{x3} = -C_2 \sin q + K_1 U_3 \sin A_1$ and

$$L_{x3} = \frac{d(K_{x3})}{dq} = -C_3 \cos q + L_1 U_3 \sin A_1 + K_1^2 U_3 \cos A_1$$

$\hspace{12cm}$ (48)

$$\ddot{Y}_3 = \ddot{q}K_{y3} + \dot{q}L_{y3}$$

where, $K_{y3} = -C_2 \cos q + K_1 U_3 \cos A_1$ and

$$L_{y3} = \frac{d(K_{y3})}{dq} = -C_3 \sin q + L_1 U_3 \cos A_1 - K_1^2 U_3 \sin A_1$$

$\hspace{12cm}$ (49)

For the **rocker 1a**,

$$\ddot{X}_4 = \ddot{q}K_{x4} + \dot{q}^2 L_{x4}$$

where, $K_{x4} = -K_2 U_4 \sin A_2$ and $\quad L_{x4} = \frac{d(K_{x4})}{dq} = -L_2 U_4 \sin A_2 - K_2^2 U_4 \cos A_2$ $\hspace{1cm}$ (50)
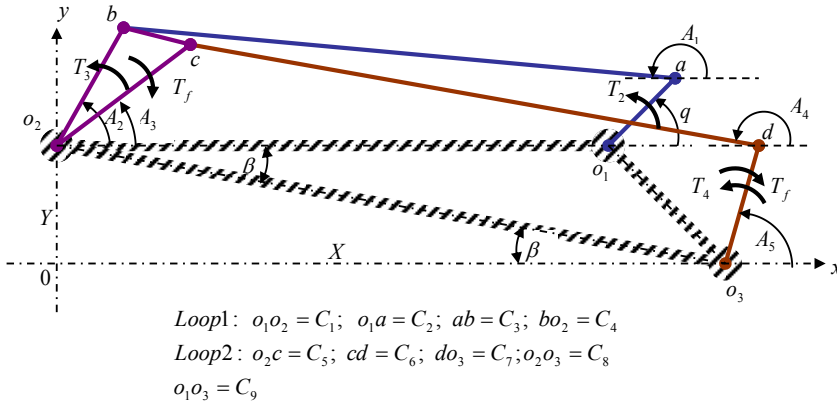
$$\ddot{Y}_4 = \ddot{q}K_{y4} + \dot{q}^2 L_{y4}$$

where, $K_{y4} = -K_2 U_4 \cos A_2$ and $L_{y4} = \dfrac{d(K_{y4})}{dq} = L_2 U_4 \cos A_2 - K_2^2 U_4 \sin A_2$ (51)

For the **rocker 1b**,

$$\ddot{X}_5 = \ddot{q}K_{x5} + \dot{q}^2 L_{x5}$$

where, $K_{x5} = -K_3 U_5 \sin A_3$ and $L_{x5} = \dfrac{d(K_{x5})}{dq} = -L_3 U_5 \sin A_3 + K_3^2 U_5 \cos A_3$ (52)

$$\ddot{Y}_5 = \ddot{q}K_{y5} + \dot{q}^2 L_{y5}$$

where, $K_{y5} = K_3 U_5 \cos A_3$ and $L_{y5} = \dfrac{d(K_{y5})}{dq} = L_3 U_5 \cos A_3 - K_3^2 U_5 \sin A_3$ (53)

For the **connecting link 2**,

$$\ddot{X}_6 = \ddot{q}K_{x6} + \dot{q}^2 L_{x6}$$

where, $K_{x6} = -K_3 C_5 \sin A_3 - K_4 U_6 \sin A_4$

$$L_{x6} = \dfrac{d(K_{x6})}{dq} = -L_3 C_5 \sin A_3 - K_3^2 C_5 \cos A_3 - L_4 U_6 \sin A_4 - K_4^2 U_6 \cos A_4$$ (54)

$$\ddot{Y}_6 = \ddot{q}K_{y6} + \dot{q}^2 L_{y6}$$

where, $K_{y6} = K_3 C_5 \cos A_3 - K_4 U_6 \cos A_4$

$$L_{y6} = \dfrac{d(K_{y6})}{dq} = L_3 C_5 \cos A_3 - K_3^2 C_5 \sin A_3 - L_4 U_6 \cos A_4 + K_4^2 U_6 \sin A_4$$ (55)

For the **rocker 2**,

$$\ddot{X}_7 = \ddot{q}K_{x7} + \dot{q}^2 L_{x7}$$

where, $K_{x7} = -K_5 U_7 \sin A_5$ and $L_{x7} = \dfrac{d(K_{x7})}{dq} = -L_5 U_7 \sin A_5 - K_5^2 U_7 \cos A_5$ (56)

$$\ddot{Y}_7 = \ddot{q}K_{y7} + \dot{q}^2 L_{y7}$$

where, $K_{y7} = K_5 U_7 \cos A_5$ and $L_{y7} = \dfrac{d(K_{y7})}{dq} = L_5 U_7 \cos A_5 - K_5^2 U_7 \sin A_5$ (57)

2.3   Kinetostatic Models

These are the models of the dynamic, pin-joint and reactive forces obtained as follows:

(a) **Dynamic Force Model**: The dynamic force models are required for the mechanism dynamic force analysis (Doughty, 1988). The models establish relations for the applied moments described in Figure 3 using energy method as follows:

$Loop1: \; o_1 o_2 = C_1; \; o_1 a = C_2; \; ab = C_3; \; bo_2 = C_4$
$Loop2: \; o_2 c = C_5; \; cd = C_6; \; do_3 = C_7; o_2 o_3 = C_8$
$o_1 o_3 = C_9$

Figure 3: Force diagram for the dual crank-rocker mechanism

The Eksergian's energy equation of motion for the two four-bar linkages are, separately, defined as,

$$\phi(q)\ddot{q} + \Phi(q)\dot{q}^2 = Q_1$$
(58)

$$\psi(q)\ddot{q} + \Psi(q)\dot{q}^2 = Q_2 \qquad (59)$$

In (58) and (59), $\phi(q)$ and $\psi(q)$ are the generalized inertia for the systems, $\Phi(q)$ and $\Psi(q)$ are the generalized centripetal coefficients for the systems, and Q_1 and Q_2 are the generalized static moments for the systems. Also, q, $\dot{q}$ and $\ddot{q}$ are the angular position, velocity and acceleration of the input crank of the mechanism. The kinetostatics analysis assumes that $\dot{q}$ is constant giving rise to $\ddot{q}$ being equal to zero. Hence, (58) and (59) reduce to,

$$\Phi(q)\dot{q}^2 = Q_1 \qquad (60)$$

$$\Psi(q)\dot{q}^2 = Q_2 \qquad (61)$$

The expressions required to estimate the coefficients in (58), (59), (60) and (61) are derived as follows:

The total kinetic energy of the two four-bar mechanisms are given as,

$$(KE)^1 = (KE)_2 + (KE)_3 + (KE)_4 \qquad (62)$$

$$(KE)^2 = (KE)_5 + (KE)_6 + (KE)_7 \qquad (63)$$

For the **crank**,

$$(KE)_2 = 0.5 I_2 \dot{q}^2 \qquad (64)$$

For the **connecting Link 1**,

$$(KE)_3 = 0.5\left(I_3 \dot{A}_1^2 + M_3 V_3^2\right) = 0.5\left(I_3 K_1^2 \dot{q}^2 + M_3 V_3^2\right) \qquad (65)$$

For the **rocker 1a**,

$$(KE)_4 = 0.5 I_4 \dot{A}_2^2 = 0.5 I_4 K_2^2 \dot{q}^2 \qquad (66)$$

For the **rocker 1b**,

$$(KE)_5 = 0.5 I_5 \dot{A}_3^2 = 0.5 I_5 K_3^2 \dot{q}^2 \tag{67}$$

For the **connecting link 2**,

$$(KE)_6 = 0.5\left(I_6 \dot{A}_4^2 + M_6 V_6^2\right) = 0.5\left(I_6 K_4^2 \dot{q}^2 + M_6 V_6^2\right) \tag{68}$$

For the **rocker 2**,

$$(KE)_7 = 0.5 I_7 \dot{A}_5^2 = 0.5 I_7 K_5^2 \dot{q}^2 \tag{69}$$

Substitution of (64), (65) and (66) into (62) yields, for the first four-bar linkage, yields

$$(KE)^1 = 0.5\phi(q)\dot{q}^2 \text{ , where, } \phi(q) = I_2 + I_3 K_1^2 + M_3 V_3^2 + I_4 K_2^2 \tag{70}$$

Also, substitution of (67), (68) and (69) into (63) yields, for the second four-bar linkage, yields

$$(KE)^2 = 0.5\psi(q)\dot{q}^2 \text{ , where, } \psi(q) = I_5 K_3^2 + I_6 K_4^2 + M_6 V_6^2 + I_7 K_5^2 \tag{71}$$

Differentiating $\phi(q)$ and $\psi(q)$ with respect to q, respectively, yields,

$$\frac{d\phi(q)}{dq} = 2\left(I_3 K_1 L_1 + M_3 V_3 + I_4 K_2 L_2\right) \tag{72}$$

$$\frac{d\psi(q)}{dq} = 2\left(I_5 K_3 L_3 + I_6 K_4 L_4 + M_6 V_6 + I_7 K_5 L_5\right) \tag{73}$$

Therefore,

$$\Phi(q) = 0.5 \frac{d\phi(q)}{dq} = I_3 K_1 L_1 + M_3 V_3 + I_4 K_2 L_2 \tag{74}$$

$$\Psi(q) = 0.5 \frac{d\psi(q)}{dq} = I_5 K_3 L_3 + I_6 K_4 L_4 + M_6 V_6 + I_7 K_5 L_5 \tag{75}$$

From the virtual work of the system, the generalized static force of the two four bar linkages are given as,

$$Q_1 = \frac{\delta w_1}{\delta q} = T_2 + T_3 K_2 - T_{f3} K_2 \tag{76}$$

$$Q_2 = \frac{\delta w_2}{\delta q} = T_3 K_3 - T_f K_3 + T_4 K_5 - T_{f4} K_5 \tag{77}$$

Therefore, substitution of (74) and (76) into (60) and noting that $T_{f3} = mT_3$, $0 \le m < 1$, where m is the proportion of the output torque that is used to overcome contact friction between the wiper and the windscreen known as the contact friction loss factor, yields,

$$\left(I_3 K_1 L_1 + M_3 V_3 + I_4 K_2 L_2 \right) \dot{q}^2 = T_2 + T_3 K_2 - T_{f3} K_2 = T_2 + T_3 K_2 (1-m)$$

$$or$$

$$T_3 = \frac{1}{K_2(1-m)} \left[\left(I_3 K_1 L_1 + M_3 V_3 + I_4 K_2 L_2 \right) \dot{q}^2 - T_2 \right] \tag{78}$$

Also, substitution of (75) and (77) into (61) and noting that $T_{f4} = mT_4$, $0 \le m < 1$, yields,

$$\left(I_5 K_3 L_3 + I_6 K_4 L_4 + M_6 V_6 + I_7 K_5 L_5 \right) \dot{q}^2 = T_3 K_3 - T_{f3} K_3 + T_4 K_5 - T_{f4} K_5$$

$$= T_3 K_3 (1-m) + T_4 K_5 (1-m)$$

$$or$$

$$T_4 = \frac{1}{K_5(1-m)} \left[\left(I_5 K_3 L_3 + I_6 K_4 L_4 + M_6 V_6 + I_7 K_5 L_5 \right) \dot{q}^2 - T_3 (1-m) \right] \tag{79}$$

Note that T_3 and T_4 are the unknown output torque at rockers 1 and 2 and they can be estimated using the expressions in (78) and (79), respectively.

The torque ratio or mechanical advantage has been defined as the capacity of a mechanism to transmit torque (Erdman et al, 1984a, 1984b). It is the ratio of the output torque to the input torque. Thus, from (78) and (79), the torque ratios for the two four-bar linkages in the mechanism and the mechanism itself, assuming no bearing friction, may be evaluated using the following expressions.

$$(TR)_1 = \frac{T_3}{T_2} = \frac{1}{T_2 K_2 (1-m)} \left[\left(I_3 K_1 L_1 + M_3 V_3 + I_4 K_2 L_2 \right) \dot{q}^2 - T_2 \right]$$
(80)

$$(TR)_i = \frac{T_4}{T_3} = \frac{1}{T_3 K_5 (1-m)} \left[\left(I_5 K_3 L_3 + I_6 K_4 L_4 + M_6 V_6 + I_7 K_5 L_5 \right) \dot{q}^2 - T_3 (1-m) \right]$$
(81)

$$(TR)_2 = (TR)_1 (TR)_i = \left(\frac{T_3}{T_2} \right) \left(\frac{T_4}{T_3} \right) = \frac{T_4}{T_2}$$
(82)

However, due to power loss in friction at bearing contact surfaces the torque ratio would be reduced by a factor, η, known as the transmission efficiency. If this is considered in the analysis, the actual values of the torque ratios will therefore be obtained using expressions: $(TR)_1 = \eta T_3 / T_2$, $(TR)_i = \eta T_4 / T_3$ and $(TR)_2 = \eta T_4 / T_2$

(b)**Pin-joint Force Model**: The pin-joint force model is required for analysis of the pin-joint or internal forces. From force equilibrium principle (Doughty, 1988) and component or free-body diagrams of the mechanism (Figures 4 to 9), the pin-joint force model is derived as follows:

The equilibrium of the **crank** (Figure 4) gives,

$$F_1 - F_3 = M_2 \ddot{X}_2$$
(83)

$$F_2 - F_4 = M_2 \ddot{Y}_2$$
(84)

$$T_2 + F_3 C_2 \sin q - F_4 C_2 \cos q = I_2 \ddot{q}$$
(85)

The equilibrium of the **connecting link 1** (Figure 5) gives,

$$F_3 - F_5 = M_3 \ddot{X}_3$$
(86)

$$F_4 - F_6 = M_3 \ddot{Y}_3$$
(87)

$$F_5 C_3 \sin A_1 + F_6 C_3 \cos A_1 = I_3 \ddot{A}_1$$
(88)
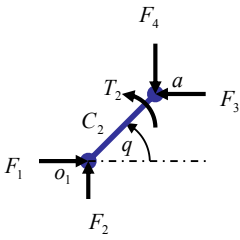
Figure 4: Free-body diagram of the crank
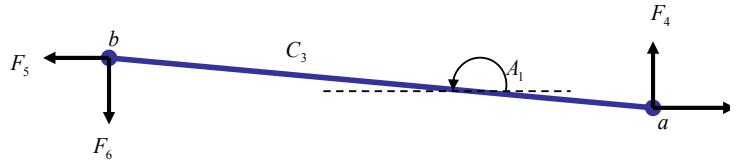
Figure 5: Free-body diagram of the connecting link 1

The equilibrium of the **rocker 1a** (Figure 6) gives,

$$F_5 - F_7 = M_4 \ddot{X}_4 \tag{89}$$

$$F_6 - F_8 = M_4 \ddot{Y}_4 \tag{90}$$

$$T_3 - T_f - F_5 C_4 \sin A_2 + F_6 C_4 \cos A_2 = I_4 \ddot{A}_2 \tag{91}$$

The equilibrium of the **rocker 1b** (Figure 7) gives,

$$F_9 - F_7 = M_5 \ddot{X}_5 \tag{92}$$

$$F_{10} - F_8 = M_5 \ddot{Y}_5 \tag{93}$$

$$T_3 - T_f - F_9 C_5 \sin A_3 + F_{10} C_5 \cos A_3 = I_5 \ddot{A}_3 \tag{94}$$
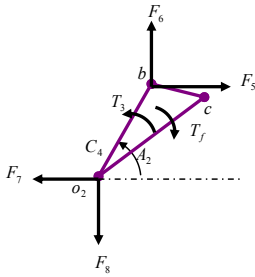
Figure 6: Free-body diagram of rocker 1a
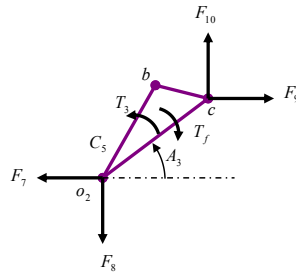
Figure 7: Free-body diagram of the rocker 1b

The equilibrium of the **connecting link 2** (Figure 8) gives,

$$F_{11} - F_9 = M_6 \ddot{X}_6 \tag{95}$$

$$F_{12} - F_{10} = M_6 \ddot{Y}_6 \tag{96}$$

$$F_{11}C_6 \sin A_4 + F_{12}C_6 \cos A_4 = I_6 \ddot{A}_4 \tag{97}$$

The equilibrium of the **rocker 2** (Figure 9) gives,

$$F_{13} - F_{11} = M_7 \ddot{X}_7 \tag{98}$$

$$F_{14} - F_{12} = M_7 \ddot{Y}_7 \tag{99}$$

$$T_7 - T_f + F_{11}C_7 \sin A_5 - F_{12}C_7 \cos A_5 = I_7 \ddot{A}_5 \tag{100}$$
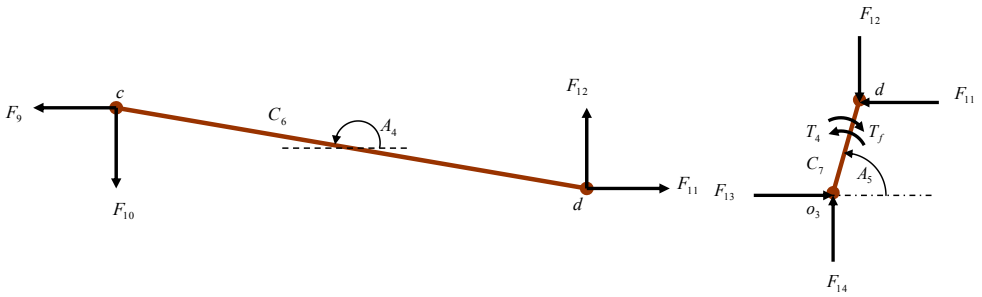
Figure 8: Free-body diagram of the connecting link 2

Figure 9: Free-body diagram of rocker 2

Equations (83) to (100) constitute eighteen linear algebraic equations to be solved for fourteen unknown components of the pin-joint forces. The linear system can be reduced to conform to the number of unknowns by ignoring (91) to (93), and the rest of the algebraic equations reset in a matrix equation of the form,

$$[\Omega]\{F\} = \{G\} \qquad (101)$$

In the matrix equation,

$$[\Omega] = \begin{bmatrix}
1 & 0 & -1 & 0 & 0 & 0 & 0 & 0 & 0 & 0 & 0 & 0 & 0 & 0 \\
0 & 1 & 0 & -1 & 0 & 0 & 0 & 0 & 0 & 0 & 0 & 0 & 0 & 0 \\
0 & 0 & C_2\sin q & -C_2\cos q & 0 & 0 & 0 & 0 & 0 & 0 & 0 & 0 & 0 & 0 \\
0 & 0 & 1 & 0 & -1 & 0 & 0 & 0 & 0 & 0 & 0 & 0 & 0 & 0 \\
0 & 0 & 0 & 1 & 0 & -1 & 0 & 0 & 0 & 0 & 0 & 0 & 0 & 0 \\
0 & 0 & 0 & 0 & C_3\sin A_1 & C_3\cos A_1 & 0 & 0 & 0 & 0 & 0 & 0 & 0 & 0 \\
0 & 0 & 0 & 0 & 1 & 0 & -1 & 0 & 0 & 0 & 0 & 0 & 0 & 0 \\
0 & 0 & 0 & 0 & 0 & 1 & 0 & -1 & 0 & 0 & 0 & 0 & 0 & 0 \\
0 & 0 & 0 & 0 & 0 & 0 & 0 & 0 & -1 & 0 & 1 & 0 & 0 & 0 \\
0 & 0 & 0 & 0 & 0 & 0 & 0 & 0 & 0 & -1 & 0 & 1 & 0 & 0 \\
0 & 0 & 0 & 0 & 0 & 0 & 0 & 0 & 0 & 0 & C_6\sin A_4 & C_6\cos A_4 & 0 & 0 \\
0 & 0 & 0 & 0 & 0 & 0 & 0 & 0 & 0 & 0 & -1 & 0 & 1 & 0 \\
0 & 0 & 0 & 0 & 0 & 0 & 0 & 0 & 0 & 0 & 0 & -1 & 0 & 1 \\
0 & 0 & 0 & 0 & 0 & 0 & 0 & 0 & 0 & 0 & C_7\sin A_5 & -C_7\cos A_5 & 0 & 0
\end{bmatrix} \quad (102)$$

$$\{F\} = \{F_1 \quad F_2 \quad F_3 \quad F_4 \quad F_5 \quad F_6 \quad F_7 \quad F_8 \quad F_9 \quad F_{10} \quad F_{11} \quad F_{12} \quad F_{13} \quad F_{14}\}^T \qquad (103)$$

and

$$\{G\} = \{G_1 \quad G_2 \quad G_3 \quad G_4 \quad G_5 \quad G_6 \quad G_7 \quad G_8 \quad G_9 \quad G_{10} \quad G_{11} \quad G_{12} \quad G_{13} \quad G_{14}\}^T \qquad (104)$$

Note that $[\Omega]$ is a $14x14$ matrix of system geometric parameters; $\{F\}$ is a $14x1$ vector of unknown components of the pin-joint forces acting on the links of the mechanism; and $\{G\}$ is a $14x1$ vector of known components of inertia forces and moments acting on the various links of the mechanism. For kinetostatic analysis, $\dot{q}$ is constant and $\ddot{q}$ is zero, and therefore, the elements of $\{G\}$, as defined in linear algebraic equations, may be obtained from, $G_1 = M_2 L_{x2}\dot{q}^2$; $G_2 = M_2 L_{y2}\dot{q}^2$; $G_3 = T_2$; $G_4 = M_3 L_{x3}\dot{q}^2$; $G_5 = M_3 L_{y3}\dot{q}^2$; $G_6 = I_3 L_1 \dot{q}^2$; $G_7 = M_4 L_{x4}\dot{q}^2$; $G_8 = M_4 L_{y4}\dot{q}^2$; $G_9 = M_6 L_{x6}\dot{q}^2$; $G_{10} = M_6 L_{y6}\dot{q}^2$; $G_{11} = I_2 L_4 \dot{q}^2$; $G_{12} = M_7 L_{x7}\dot{q}^2$; $G_{13} = M_7 L_{y7}\dot{q}^2$; and $G_{14} = (m-1)T_7 + I_2 L_5 \dot{q}^2$.

The solution of the matrix equation by any known method for linear system (Chapra et al, 1998, Cheney et al, 1999, Rajasekaran, 2003) would result to estimate the pin-joint forces, $\{F\}$.

(c) **Reactive Force model**: The reactive force models are required for the mechanism reactive force analysis. The models establish relations for the reactive forces and moments acting on the fixed frame described in Fig. 11 as follows:

The equilibrium of the **fixed frame** (Figure 10) gives,

$$R_1 = F_1; \quad R_2 = F_2; \text{ and } T_{R1} = 0 \qquad (105)$$

$$R_3 = F_7; \quad R_4 = F_8; \text{ and } T_{R2} = 0 \qquad (106)$$

$$R_5 = F_{13}; \quad R_6 = F_{14}; \text{ and } T_{R3} = 0 \qquad (107)$$
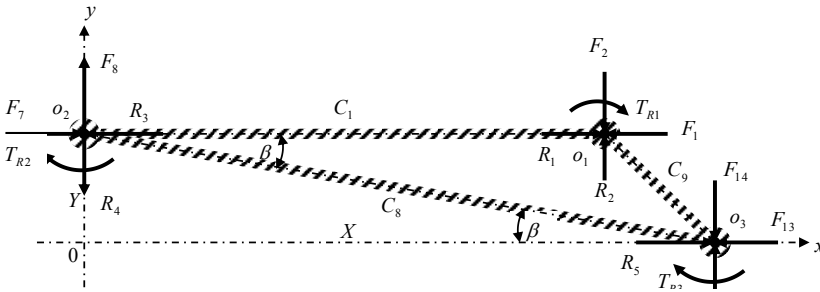
Figure 10: Free-body diagram of the fixed frame

2.4 **Simulations for Mechanism Kinematic and Kinetostatic Characterization**

Numerical experiments or simulations were conducted in MS Excel environment in order to obtain numerical data for the mechanism kinematic and kinetostatic characterization, and also, for the evaluation of its power transmission capability. These kinematic and kinetostatic data were obtained through solutions of the kinematic and kinetostatic models and experimentation with the models under the following conditions.

The linkage dimensions as obtained through direct measurements of the various links are given in Table 1. The section properties of the linkages were also obtained as given in Table 2.

The kinematic and kinetostatic data were obtained under the condition that the crank size is set at $C_2 = 0.041 m$, its angular speed is maintained constant at $\dot{q} = 0.0\, rpm$, its acceleration is set at $\ddot{q} = 0.0\, rpm$, and its torque is maintained constant at $T_2 = 80\, Nm$. This condition is used to determine static data. In each case, the crank rotations or angular positions were set in the range from 0 to 360 degrees, distributed as given in Table 3 together with the graphically obtained initial guesses for the rotations or angular positions of other links as required for the position analysis. The friction factor due to the contact of the wiper with the windscreen and the power loss factor due to bearing friction at pin-joint were set at $m = 0.0$ and $\eta = 1.0$ respectively.

The above conditions for kinematic and kinetostatic analysis were maintained as basic in parametric analysis, but variation of the crank angular speed ($\dot{q}$) in the range from 0 to 3000 rpm; the crank torque (T_2) in the range from 0 to 1000 Nm; and the windscreen-wiper contact friction factor (m) in the range from 0 to 0.90 were used to study the effect of the input speed, input torque and friction factor of the mechanism on its power transmission capability at different crank angular positions. The ANOVA with repeated measures

(Frank et al, 1995) were used to test for significance of these variations, with the null hypothesis that the crank angular speed, torque and the wiper contact friction factor have no significant influence the transmission ratios of the mechanism.

Table 1: Linkage Dimensions

LINK	NOTATION	DIMENSION	UNIT
Fixed frame 1($o_1 o_2$)	C_1	0.4580	m
Crank ($o_1 a$)	C_2	0.0410	m
Connecting link 1 (ab)	C_3	0.4500	m
Rocker 1a (bo_2)	C_4	0.0520	m
Rocker 1b ($o_2 c$)	C_5	0.0490	m
Connecting link 2 (cd)	C_6	0.5170	m
Rocker 2 (do_3)	C_7	0.0530	m
Fixed frame 2 ($o_2 o_3$)	C_8	0.521	m
$o_1 o_3$	C_9	0.0920	m
bc	C_{10}	0.0180	m
Inner radii of connecting links	$r_3 = r_6$	0.0064	m
Angle Between bo_2 and $o_2 c$	α	20.0000	deg
Angle between $o_1 o_2$ and $o_2 o_3$	β	8.0000	deg

Table 2: Section properties of links of the mechanism

Link	Mass(Kg)	Moment of Inertia($Kg\,m^2$)
2	0.0785	4.40E-05
3	0.0882	1.49E-03
4	0.0737	6.64E-05
5	0.0737	5.90E-05
6	0.1595	3.56E-03
7	0.1833	1.66E-02

Table 3: Crank positions and initial guesses for the angular positions of other links

q	A_1	A_2	A_3	A_4	A_5
0	3	27	10	7	15
30	1	36	18	9	12
60	1	57	39	7	50
90	1	82	62	7	70
120	3	104	83	7	89
150	3	127	106	6	114
180	5	131	109	7	109
210	72	119	102	3	97
240	11	103	83	6	98

Analysis of Rocker Mechanism for Automobile Windscreen Wiper Applications

270	12	81	63	6	77
300	10	61	44	5	53
330	6	28	9	6	19
360	3	27	10	7	15

3. RESULTS AND DISCUSSION

Based on the stated assumptions and the specified conditions for numerical experiments, the obtained numerical results and analysis of results are given and also discussed as follows:

3.1 Kinematic Data

Once again, kinematics refers to the study of motion of a body or a system of bodies without consideration of the forces and moments that are responsible to the motion. In this study, therefore, the motion of the mechanism and its components is characterized by the kinematic variables. These variables include the angular positions, A, velocity coefficients, K, and the velocity coefficient derivatives, L. They were obtained in numerical experiments through solutions of the derived linear models for kinematics of the mechanism and its linkage mass centers at different crank positions. The normalized results, using the expressions, $q/|q|_{max}$, for the crank positions, $A/|A|_{max}$, for the angular positions of other links, $K/|K|_{max}$, for the velocity coefficients, and $L/|L|_{max}$, for the velocity coefficient derivatives, are given in Figures 11 through 16, while the maximum and minimum values of these kinematic variables and the corresponding crank positions are given in Tables 4 through 7.

(a) **Motion of Connecting Link 1**: The connecting link 1 of the mechanism couples the rotating crank to the oscillating rocker 1, and therefore, performs a general rigid body motion, characterized by the combined oscillatory and reciprocating type of motion. The normalized variation of its angular motion with respect to crank angular position is given in Figure 11, whereas, the path traced by its mass center in the course of its motion is not circular like those of the crank and the rockers, but as describe in a coupler curve given in Figure 12a. Also, the trace of mass center velocity and acceleration are respectively given in Figures 12b and 12c, whereas, the normalized variation of components of the mass center motion with respect to crank angular position is given in Figure 12d. It is shown that, in one revolution of the crank, the angular position of the connecting link 1 first decreased to its minimum value, then increased to its maximum value, and finally,

decreased to its initial value. The angular velocity coefficient increased to its maximum value, then decreased to its minimum value and finally increased to its initial value. The angular acceleration also increased to it maximum value, then decreased to its minimum value, and finally increased to it initial values. The maximum and minimum values of the angular motion and the corresponding crank angular position are given in Table 4. The described angular motion of this link is typical of that of similar link in the crank-rocker mechanism (Erdman et al, 1984a, 1984b) and is well described by the derived kinematic models.
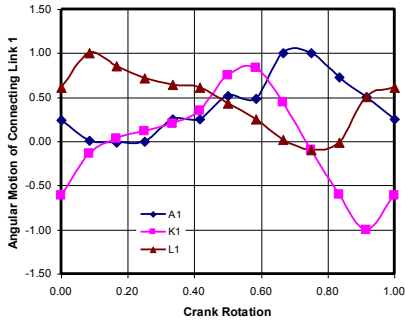
(a)

Figure 11: Normalized variation of angular motion of connecting Link 1 with respect to the crank rotation

(b)

(c)

(d)

(e)
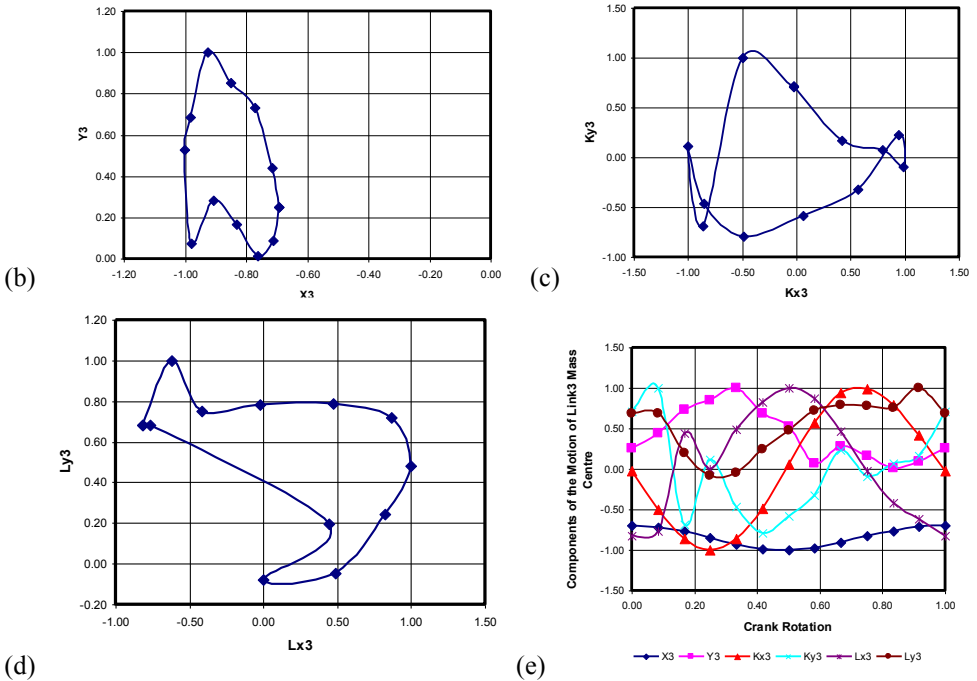
Figure 12: Normalized coupler curve of connecting Link 1(a) mass center position; (b) mass center velocity; (d) mass center acceleration; and (e) the variation of component motion of its mass center with respect to the crank rotation

Table 4: Maximum and minimum values of angular motion of the connecting link 1 and corresponding crank position

	$A_1 (rad)$	K_1	L_1
Absolute value of maximum motion	0.2196	0.1356	0.2318
Crank angular position (deg)	270	300	30
Absolute value of minimum motion	0.0006	0.0047	0.0022
Crank angular position (deg)	90	60	270

(b) **Motion of Rocker 1**: The rocking motion of one of the wiper blade is transmitted by the rocker 1 through its revolute pin. Rocker 1 is, therefore, an output triangular link, with its two active sides referred to as rocker 1a and rocker 1b, and performs a rocking motion about a fixed axis characterized by an oscillatory type of motion.   The normalized variations of their respective angular motions with respect to crank angular positions are given in Figure 13. In both cases, it is shown that, in one revolution of the crank after an approximate short dwell, the angular positions increased to its maximum value, and then, decreased to its initial value after an approximate short dwell. The angular velocity first decreased to its minimum value, then increased to its maximum value, and finally, decreased to its initial value in a sinusoidal wave pattern. The angular acceleration first decreased to its minimum value, then increased to its maximum value, and then, decreased its initial value after an approximate short dwell. The maximum and minimum values of the angular motion and the corresponding crank position are given in Table 5.   The described angular motion of this link is characteristic of rocking or oscillatory motion (Erdman et al, 1984a, 1984b) and is well described by the derived kinematic models.
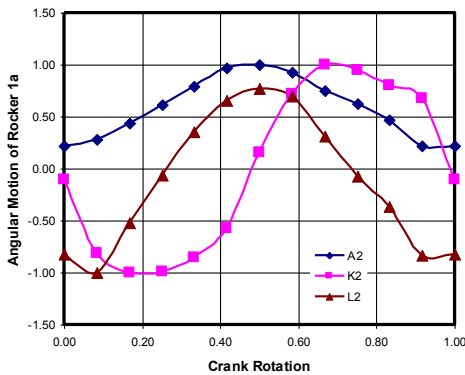
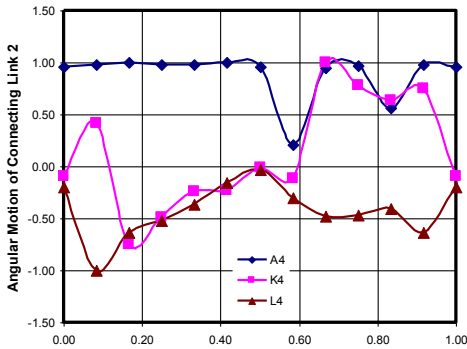(a)   (b)
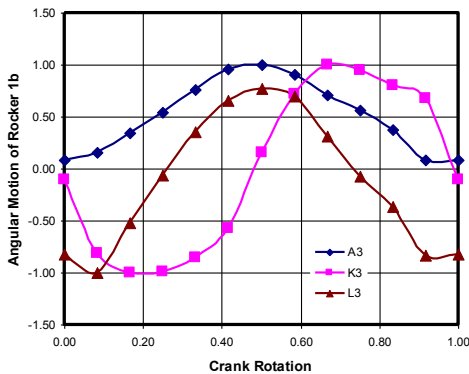
**Figure 13: Normalized variation of angular motion of the (a) rocker 1a and (b) rocker 1b with respect to crank rotation**

Table 5: Maximum and minimum values of motion of the rocker 1 and corresponding crank position

(I) **Rocker 1a**			
Parameter description	$A_2\,(rad)$	K_2	L_2
Absolute maximum motion	2.2784	0.8099	1.6938
Crank angular position (deg)	180	240	30
Absolute minimum motion	0.5004	0.0805	0.1064
Crank angular position (deg)	30	0 (360)	90
(II) **Rocker 1b**			
Parameter Description	$A_3\,(rad)$	K_3	L_3
Absolute maximum motion	1.9293	0.8099	1.6938
Crank angular position (deg)	180	240	30
Absolute minimum motion	0.1513	0.0805	0.1064
Crank angular position (deg)	0 (360)	0 (360)	90

(c) **Motion of Connecting Link 2**: The connecting link 2 connects two rockers of different geometric dimensions, and therefore, performs a general rigid body motion that is fairly characteristic of the combined oscillatory and reciprocating type of motion. This can be seen from the graphs of the normalized variation of its angular motion with respect to the crank angular position given in Figure 14, and that of its coupler curve given in Figures 15a, 15b and 15c, with patterns that are not definite, but have combined oscillatory and reciprocating characteristics with evidence of oscillatory component motion given in Figure 15d as the sinusoidal wave form of the velocity coefficient of the mass center in the x coordinate direction. However, the maximum and minimum values its angular motion and the corresponding angular crank positions are given in Table 6.
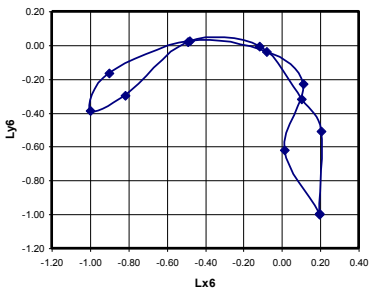
Figure 14: Normalized variation of angular motion of the connecting Link 2 with respect to the crank rotation
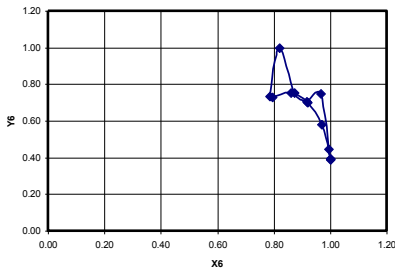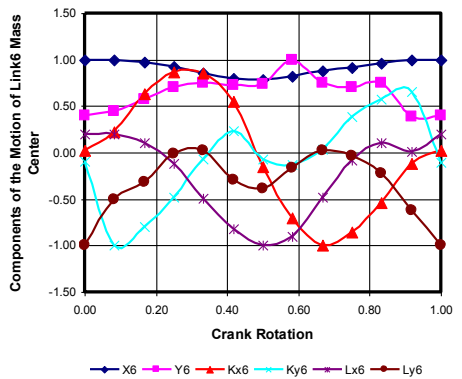

(b)
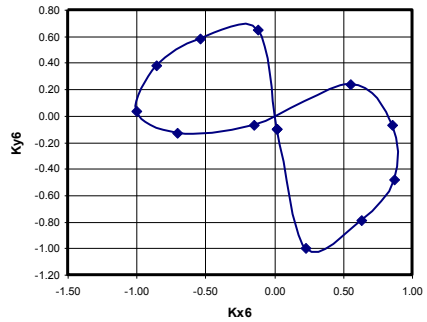
(c)

(d)

(e)

Figure 15: Normalized coupler curve of the connecting Link 2 (a) mass center position; (b) mass center velocity; (c) mass center acceleration; and (d) the variation of component motion of its mass center with respect to the crank rotation

Table 6: Maximum and minimum values of angular motion of the connecting link 2 and corresponding crank position

Parameter Description	$A_4 \left(rad \right)$	K_4	L_4
Absolute maximum motion	0.1430	0.0257	0.2227
Crank angular position (deg)	30	60	330
Absolute minimum motion	0.0298	0.0003	0.0062
Crank angular position (deg)	210	180	150

 (d) **Motion of Rocker 2**: The rocker 2 transmits, through its revolute pin, the rocking motion to the second wiper blade. It is therefore the second output link, and performs a rocking an oscillatory motion about a fixed axis. The normalized variation of the angular motion of the link with respect to the angular position of the crank is described in Fig. 16. It shown that, in one revolution of the crank, after an approximate short dwell, the angular position of the link increased to its maximum value, and then, decreased to its initial value after an approximate short dwell. The angular velocity first increased to its maximum value, then decreased to its minimum value, and finally, increased to its initial value in a sinusoidal wave pattern. The angular acceleration first decreased to its minimum value, and then, increased to its initial value. The observed motion, with exception of its angular position, is in opposite sense to that of rocker 1. However, its motion is similarly characteristic of the rocking or oscillatory motion (Erdman et al, 1984a, 1984b) and is well described by the derived kinematic models.
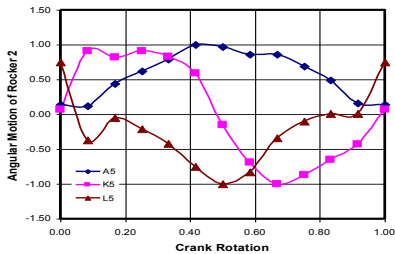
Figure 16: Normalized variation of angular motion of the rocker 2 with respect to crank rotation

Table 7: Maximum and minimum values of angular motion of the Rocker 2 and corresponding crank positions

	$A_5\,(rad)$	K_5	L_5
Absolute maximum motion	1.9711	0.7708	1.1716
Crank angular position (deg)	150	240	180
Absolute minimum motion	0.2338	0.0520	0.0063
Crank angular position (deg)	30	0 (360)	270

3.2 **Kinetostatic Data**

Kinetostatics refers to the study of forces and moments that are responsible to the motion of a body or system of bodies. In this study, therefore, the forces and moments that are responsible for the motion of the mechanism are the kinetostatic variables. These variables are the transmitted or output torques, transmission ratios, pin-joint or internal and the reactive forces. Knowledge of these forces and moments are required to enable the assessment of stresses and strain in the mechanism linkages and also to enable these linkages to be sized. Whereas, that of the transmission ratio or mechanical advantage is require to enable the evaluation of the power transmission capability of the mechanism. They were obtained in numerical experiments through solutions of the derived linear models for kinetostatics of the mechanism at different crank positions. The normalized results obtained using the expressions, $q/|q|_{\max}$, for the crank angular positions; $T/|T|_{\max}$, for the transmitted or output torques; $TR/|TR|_{\max}$, for the transmission ratios of the mechanism; $F/|F|_{\max}$, for the pin-joint forces acting on the links; and $R/|R|_{\max}$, for the reactive forces acting on the fixed frame; are given in Figs 17 and 18, while the maximum and minimum values of these kinematic variables and the corresponding crank positions are given in Tables 8 and 9.

(a) **Transmitted Torque and Transmission Ratio**: The torques T_3 and T_4 transmitted from the crank through the connecting links to the rockers, are expected to be of the magnitude that can overcome both the contact and bearing friction, and also to ensure the mobility of the linkages at different crank angular positions. They are indicators of the power output of the mechanism. On the other hand, the transmission ratios, $TR_1 = T_3/T_2$, $TR_i = T_4/T_3$ and $TR_2 = T_4/T_2$ are indicators of the mechanism's capacity to transmit

torque or power from the crank through its connecting links to the rockers. For the mechanism studied, the normalized variations of the transmitted torques and transmission ratios with respect to the crank angular positions are given in Figures. 17a and 17b, respectively. The maximum and minimum values of these variables and the corresponding crank angular positions are given in Table 8. It is observed that, in one revolution of the crank, both torques and transmission ratios decreased from their maximum values to a set of fairly constant minimum values before their values suddenly increased, and then, decreased to another set of fairly constant minimum values, and finally, increased to their initial values. However, intermediate transmission ratio, TR_i has different characteristics, with no definite pattern. The high values of these variables, which occur at the initial, middle and the final position in one revolution of the crank, are evidence of the occurrence of locking effect at the dead ends, and at the peak of the motion of the rockers. At these points, high torques and transmission ratios are expected in order to ensure continuity in the mobility of the linkages. However, they contribute to the high torsional stresses in the revolute pins of the rockers, and therefore, are to be considered in the stress analyses of these pins.


(a)   (b)
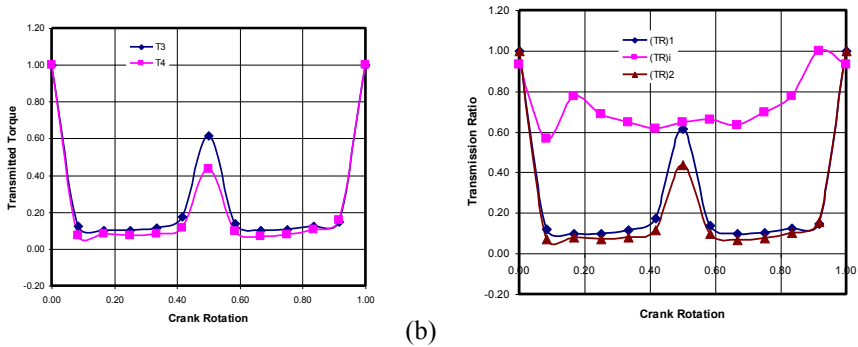
Figure 17: Normalized variation of the (a) transmitted torques and (b) transmission ratios with respect to crank angular positions

Table 8: Maximum and minimum values of torque and torque ratios, and corresponding crank positions

Parameter Description	Transmitted Torque		Transmission Ratio		
	$T_3 \, (Nm)$	$T_4 \, (Nm)$	$(TR)_1$	$(TR)_i$	$(TR)_2$
Absolute maximum values	994.0	1537.0	12.43	1.66	19.21
Crank angular positions (deg)	0 (360)	0 (360)	0 (360)	0 (360)	0 (360)

| Absolute Minimum values | 99.0 | 104.0 | 1.23 | 0.94 | 1.30 |
| Crank angular positions (deg) | 240 | 240 | 240 | 30 | 240 |

(b) **Pin-Joint and Reactive Forces**: The pin-joint ($F_{i,j}$) and reactive ($R_{i,j}$) forces are transmitted to the linkages and the fixed frame, respectively, and act to subject them to axial stresses. The normalized variations of these forces with respect to the crank angular position are given in Fig. 18. Whereas, the maximum and minimum values of these forces and the corresponding crank angular positions are given in Table 9. As in the transmitted torques, the high values of these variables, which occur at the initial, middle and the final position in one revolution of the crank, are evidence of the occurrence of locking effect at the dead ends, and at the peak of the motion of the rockers. At these points, high forces induce high axial stresses in the linkages and therefore call for consideration in stress analyses of these linkages. Generally, under dynamic conditions, the induced torsional and axial stresses may repeatedly increase and decrease at equal rate with the motion of the linkages. This could lead to fatigue of these linkages. Therefore, evaluation of the fatigue strength of these linkages is required to ensure their reasonable service life.

(a)   (b)
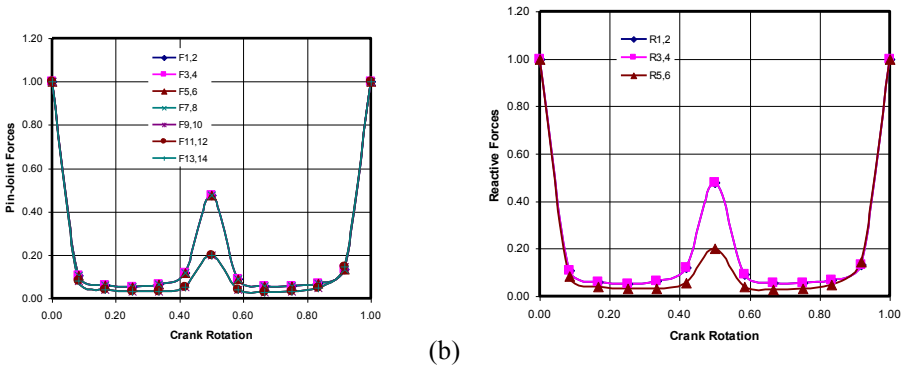
Figure 18: Normalized variation of the (a) pin-joint forces and (b) reactive forces with respect to crank angular positions

Table 9: Maximum and minimum values of pin-joint and reactive forces, and corresponding crank positions

Parameter Description	$F_{1,2}\left(R_{1,2}\right)$	$F_{3,4}$	$F_{5,6}$	$F_{7,8}\left(R_{3,4}\right)$	$F_{9,10}$	$F_{11,12}$	$F_{13,14}\left(R_{5,6}\right)$
Absolute maximum forces (N)	36231.8	36231.8	36231.8	36231.8	70998.8	70998.8	70998.8
Crank position (deg)	0 (360)	0 (360)	0 (360)	0 (360)	0 (360)	0 (360)	0 (360)
Absolute minimum forces (N)	1951.2	1951.2	1951.2	1951.2	2029.0	2029.0	2029.0
Crank position (deg)	90	90	90	90	240	240	240

3.3 **Parametric Data**

How the input speed, input torque and the contact friction as in windscreen wiper applications influence the power transmission capability of the mechanism is investigated in its parametric analysis. In one revolution of the crank, the transmission ratios TR_1 and TR_2 were evaluated at different values of the input speed, input torque and contact friction that were selected within the specified range of values for the parametric analysis and at different crank angular positions. The obtained raw data were subjected to analysis of variance (ANOVA) with repeated measures [Frank et al, 1995] and the results tabulated in Tables 10 through 15. It is of interest to test the null hypotheses that the input speed, input torque and contact friction have no significant influence on the power transmission capability of the mechanism. The hypothesis is accepted for the cases of TR_2 versus $\dot{q}$ (Table 11) and TR_2 versus T_2 (Table 13), but rejected for the cases of TR_1 versus $\dot{q}$ (Table 10), TR_1 versus T_2 (Table 12), TR_1 versus m (Table 14) and TR_2 versus m (Table 15). In other words, there is no significant variation of the TR_2 with respect to $\dot{q}$ and T_2. Whereas, there is significant variation of TR_1 with respect to $\dot{q}$, T_2 m, and TR_2 with respect to m. It is also important to note that, as shown in Tables 10 through 15, there are significant variations of TR_1 and TR_2 with respect to crank rotation q even though it is not emphasized at the onset.

Table 10: Summary of ANOVA with Repeated Measures for the Case of TR_1 versus $\dot{q}$

Source of Variance	SS	df	MS	F	F_c	p
Crank Speed ($\dot{q}$)	0.0290	6	0.0048	15.4409	2.236	0.05
Crank Position (q)	0.0515	12	0.0043	13.7205	1.902	0.05
Residual	0.0225	72	0.0003			
Total	0.1030	90				

Table 11: Summary of ANOVA with Repeated Measures for the Case of TR_2 versus $\dot{q}$

Source of Variance	SS	df	MS	F	F_c	p
Crank Speed ($\dot{q}$)	0.0024	6	0.0004	0.4426	2.236	0.05
Crank Position (q)	0.0673	12	0.0056	6.2213	1.902	0.05
Residual	0.0649	72	0.0009			
Total	0.1346	90				

Table 12: Summary of ANOVA with Repeated Measures for the Case of TR_1 versus T_2

Source of Variance	SS	df	MS	F	F_c	p
Crank Torque (T_2)	0.0000169	5	0.0000034	16.0999	2.3700	0.05
Crank Position (q)	0.0000295	12	0.0000025	11.7083	1.9200	0.05
Residual	0.0000126	60	0.0000002			

Total	0.0000590	77				

Table 13: Summary of ANOVA with Repeated Measures for the case of TR_2 versus T_2

Source of Variance	SS	df	MS	F	F_c	p
Crank Torque (T_2)	0.00051	5	0.00010	0.9706	2.3700	0.05
Crank Position (q)	0.00681	12	0.00057	5.4044	1.9200	0.05
Residual	0.00630	60	0.00010			
Total	0.01361	77				

Table 14: Summary of ANOVA with Repeated Measures for the Case of TR_1 versus m

Source of Variance	SS	df	MS	F	F_c	p
Friction Factor (m)	10359.60	5	2071.92	9.6677	2.3700	0.05
Crank Position (q)	23218.41	12	1934.87	9.0282	1.9200	0.05
Residual	12858.80	60	214.31			
Total	46436.82	77				

Table 15: Summary of ANOVA with Repeated Measures for the Case of TR_2 versus m

Source of Variance	SS	df	MS	F	F_c	p
Friction Factor (m)	2463947.78	5	492789.56	7.4892	2.3700	0.05
Crank Position (q)	6411969.30	12	534330.77	8.1205	1.9200	0.05
Residual	3948021.52	60	65800.36			
Total	12823938.60	77				

4   CONCLUSION

The kinematic and kinetostatic analysis models for the crank-double rocker mechanisms have been derived based on concepts of the vector loop closure, velocity coefficients and the velocity coefficient derivatives, and on the generalized energy based equation of motion and concepts of dynamic equilibrium of forces and moments, and of virtual work, respectively.   The derived models have been subsequently used in experiments to numerically study the kinematics and kinetostatics of the mechanism. The results of the numerical experiments showed that, the kinematic and kinetostatic characteristics of the various components and loops of the mechanism are as expected. The observed rocking or oscillatory motion is characteristic of the rockers, whereas the observed combined reciprocating and oscillatory motion is characteristic of the connecting links.   There is significant variation of the linkage motion with respect to crank rotation.   In a single revolution of the crank, the magnitude of the output torque, transmission ratios, and of the pin-joint and reactive forces are relatively high at the start, middle and end of the revolution, and so is expected of the induced stresses due to these forces and moments, respectively.   The input speed, input torque and friction factor, were found to have significant influence on the power transmission capability of first loop of the mechanism; whereas, only the friction factor has significant influence on the power transmission capability of second loop of the mechanism.   It is therefore concluded that, since the derived models described the performance characteristics of the mechanism in clear terms, they are suitable for practical design and analysis of crank-double rocker mechanism and its components for automobile windscreen wiper and similar other applications, both in MS Excel and in any other mechanism analysis software environment.

5 REFERENCES

Bahgat, B. M. and Willmert, K. D. (1976)). *Finite Element Vibrational Analysis of Planar Mechanisms*, Mechanism and Machine Theory, Vol. 11, pp 47 – 71

Berkof, R. S. (1979). *The Input Torque in Linkages*, Mechanism and Machine Theory, Vol. 14, pp 61 – 73

Berkof, R. S. and Lowen, G. G. (1971). *Theory of Shaking Moment Optimization of Force-Balanced Four-bar Linkages*, Journal of Engineering for Industry, Transactions of the ASME, No. 2, pp 53 – 60

Chapra, S. C. and Canale, R. P. (1998). *Numerical Methods for Engineers with Programming and Software Applications*, 3rd Edition, Mcgraw-Hill, USA: New York

Cheney, W. and Kincaid, D. (1999). *Numerical Mathematics and Computing*, 4th Edition, Brooks and Cole publishing Company, USA: New York

Cheng, H. H. and Trang, D. T. (2006). *Object-oriented interactive mechanism design and analysis*, Engineering with Computers, Vol. 21, pp 237 – 246

Doughty, S. (1988). *Mechanics of Machines*, WIE, John Wiley and Sons Ltd, USA: New York

Erdman, A. G. and Sandor, G. N. (1984). *Advanced Mechanism Design: Analysis and Synthesis*, vol. 2, Prentice-Hall, Inc, Englewood Cliffs, USA: New Jessey

Erdman, A. G. and Sandor, G. N. (1984). *Mechanism Design: Analysis and Synthesis*, vol. 1, Prentice-Hall, Inc, Englewood Cliffs, USA: New Jessey

Erdman, A. G., Sandor, G. N. and Oakberg, R. G. (1972). *A general method for Kineto-Elastodynamic Analysis and Synthesis of Mechanisms*, Journal of Engineering for Industry, Transsactions of the ASME, No.11, pp 1193 – 1205

Frank, H and Althoen, S. C. (1995). *Statistics: Concept and Applications*, Cambridge Low Price Editions, Cambridge University Press, UK: Great Britain

Izelu, C. O. (2000). *A Computer-Aided Design Study of the Rotary Geneva Mechanism*, Journal of the National Science and Technology Forum (NSTF), Vol. 1, No. 1, pp 97 – 106

Izelu, C. O. (2002). *An Assessment of the Power Transmission Capability of the External*

Rotary Geneva Mechanism, Academy Journal of Science and Engineering, Vol. 2, No. 1, pp 82 – 101

Joskowicz, L. and Sacks, E. (1999). *Computer-Aided Mechanical Design Using Configuration Spaces*, IEEE Computer in Science and Engineering, No. 11/12 pp 14 – 21

Lowen, G. G. and Berkof, R. S. (1971). *Determination of Force-balanced Four-Bar linkages with Optimum Shaking Moment Characteristics*, Journal of Engineering for Industry, Transactions of the ASME, No. 2, pp 39 – 46

Nagchaudhuri, A. (2008). Dynamic Modeling and Analysis of a Crank Slider Mechanism, www.workingmodel.com

Nelson, D. D. and Cohen, E. (1999). *Interactive Mechanical Design Variation for Haptics and CAD*, Eurographics '99, Eurographics Association and Blackwell Publishers, Vol. 18, No. 3, pp 420 – 508

Paul, B. (1975). *Analytical Dynamics of mechanisms – A Computer Oriented Overview*, Mechanism and Machine Theory, Vol. 10, pp 481 – 507

Rajasekaran, S. (2003). *Numerical methods in Science and Engineering: A Practical Approach*, S. Chand and Company Ltd, Ram Nagar, India: New Delhi

Singhal, K. and Kesavan, H. K. (1983). *Dynamic Analysis of Mechanisms via Vector Network Model*, Mechanism and Machine Theory, Vol. 18, pp 175 – 180

Sohoni, V. N. and Haug, E. J. (1982). *A State Space Technique for Optimal Design of Mechanisms*, Transactions of the ASME, Vol. 104, No. 10, pp 792 – 798

Wang, S. L. (2008). Mechanism Simulation with Working Model, www.workingmodel.com

Wehage, R. A. and Haug, E. J. (1982). *Dynamic Analysis of Mechanical Systems with Intermittent Motion*, Transactions of the ASME, Vol. 104, No. 10, pp 778 – 784

APPENDIX: PICTURE OF THE MECHANISM IN TWO VIEWS

Analysis of Rocker Mechanism for Automobile Windscreen Wiper Applications